UDC 551.509.313:551.511.3

TESTS OF THE EFFECT OF GRID RESOLUTION IN A GLOBAL PREDICTION MODEL

M. SANKAR RAO

Institute for Space Studies, Goddard Space Flight Center, NASA, New York, N.Y.

LUDWIG UMSCHEID, JR.

Computer Applications, Inc., New York, N.Y.

ABSTRACT

Kurihara and Holloway have proposed an integration scheme that offers advantages in the problems of geophysical fluid dynamics by rigorously conserving mass and energy. We have attempted to investigate the accuracy of the Kurihara and Holloway method by numerical experiments, applying it to a problem for which an approximate analytic solution is available.

For the case in which the planetary wave number is 4, we find that with the equal-area grid and with a latitude grid spacing of 4.5°, the planetary wave is destroyed by truncation errors within 5 days. In order to achieve a solution with acceptable accuracy, in which the planetary wave character is retained for a minimum of 10 days, the grid spacing near the Pole has to be decreased by a factor of 9.

1. INTRODUCTION

In recent years, a number of stable numerical schemes that conserve total mass and energy have been proposed by various authors for the integration of the primitive equations of geophysical fluid dynamics. One such scheme is due to Kurihara and Holloway (1967). In the scheme of Kurihara and Holloway, the angular grid spacing is variable and is chosen in such a way that the area of each box is approximately constant over the whole globe. It is felt that such spacing would allow larger time steps to be taken in the global prediction models without introducing serious errors. It is the purpose of this paper to give results of tests of the Kurihara and Holloway scheme with various grid resolutions, in order to examine the errors produced by the expanded grid spacing near the Poles. For the tests, we chose a case for which an approximate analytic solution has been given by Haurwitz (1940). This case has been used also by Phillips (1959), Kurihara (1965), and Grimmer and Shaw (1967) for testing the accuracy of numerical schemes.

2. FINITE-DIFFERENCE MODEL EQUATIONS

The atmospheric model and the initial fields are the same as those described by Phillips (1959), who, for reasons discussed by Charney (1955), used the balance equation to get the initial fields. We give below only the finite-difference form of the equations using operators and symbols of Kurihara and Holloway (1967). Here ϕ is substituted for P_* in the H_1 operator and we indicate this by H_1^ϕ. Also, we use the same symbols of Kurihara (1965) for geopotential, eastward velocity, northward velocity, and the Coriolis force. Thus our finite-difference model equations are

$$\partial\phi/\partial t \sim -H_1^\phi(1),$$

$$\partial U/\partial t \sim -H_1^\phi\frac{(u_l+u_0)}{2}+(f+mu_0)\,v_0\phi_0-L_\lambda(\phi,\phi),$$

and

$$\partial V/\partial t \sim -H_1^\phi\frac{(v_l+v_0)}{2}-(f+mu_0)u_0\phi_0-L_\varphi(\phi,\phi).$$

It can be shown that the above system conserves the total sum of kinetic and potential energy over the globe, under the same boundary conditions as Kurihara (1965). However at the Poles we have not assumed calm conditions as Kurihara (1965) did, for such a condition is not necessary in this scheme for energy conservation.

3. RESULTS OF THE TEST RUNS

The details about the experiments performed are given in table 1.

For continuity purposes we give in figure 1 the initial height field, which is the same for all experiments.

In figures 2 to 7, we give for experiments 1 to 6, in that order, forecast fields at the end of the 10th day.

In the same order, in figures 8 to 13 we give the plots of kinetic and potential energies over the entire octant for the entire period of integration.

Finally, in figure 14 we give the zonal mean velocity for the first six experiments at the end of the 10th day.

As can be expected, from figures 2 to 7 we can see that progressively better results are obtained with better resolution. For $N=20$, we can see all the observations reported by Grimmer and Shaw (1967) for what they term the VDL scheme.

From figures 8 to 13, as well as from table 1, it can be observed that this scheme conserves total energy and total absolute angular momentum to a high degree of accuracy, which increases with increasing resolution. In all experiments except experiment 2, the global kinetic energy increased rapidly for the first few days and showed

TABLE 1.—*Experiments performed*

No.	Scheme	N	ΔT	$\overline{N}$	$\overline{T}$	RTE	RTAAM
1	A	20	600	210	0.4	6.39×10^{-5}	1.76×10^{-1}
2	B	20	600	210	0.8	8.80×10^{-2}	1.41×10^{-1}
3	A	36	300	666	2.5	3.34×10^{-6}	3.31×10^{-2}
4	B	36	300	666	4.4	2.92×10^{-4}	3.22×10^{-2}
5	A	48	180	1176	7.4	8.51×10^{-7}	1.50×10^{-2}
6	A	72	150	2628	18.0	2.60×10^{-7}	1.56×10^{-3}
7	A	20	60	370	2.9	4.20×10^{-5}	1.64×10^{-2}
8	A	20	40	540	5.3	1.54×10^{-8}	1.15×10^{-2}

Scheme A=leap-frog method.
Scheme B=modified Euler-backward method.
N=resolution.
$\overline{N}$=number of points over an octant.
ΔT=time step in seconds.
$\overline{T}$=total time in minutes taken by the IBM 360/95 computer for integration for a day over an octant.
RTE=range of the total energy in percent of the initial value, for the first 10-day period.
RTAAM=range of the total absolute angular momentum in percent of the initial value, for the first 10-day period.

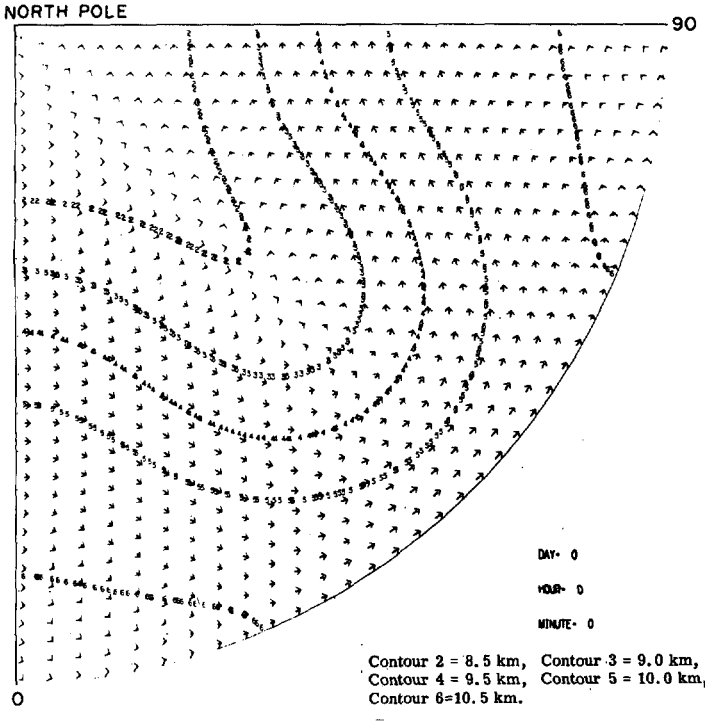

FIGURE 1.—Initial height field with wind vectors.

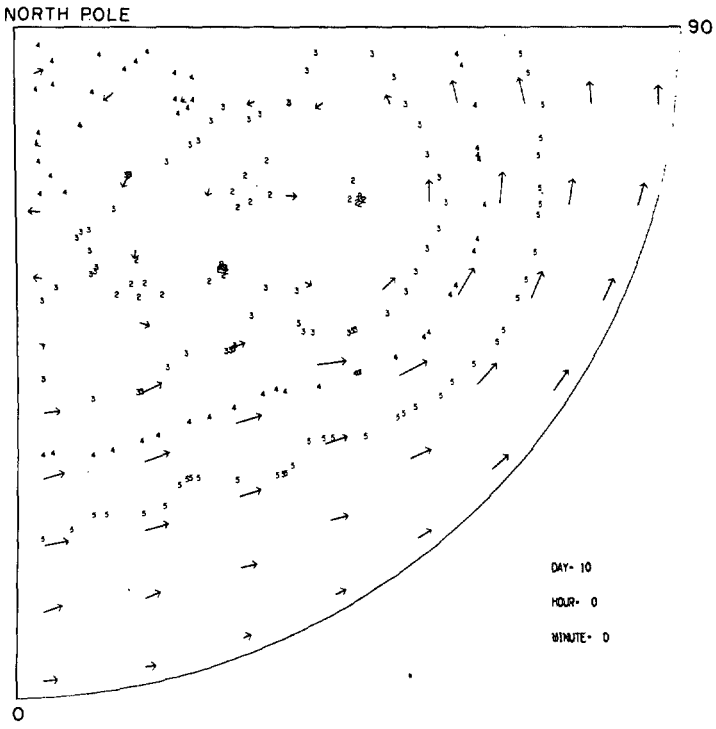

FIGURE 2.—Forecast height and wind fields at the end of the 10th day for experiment 1. Legend for contour values in figure 1.

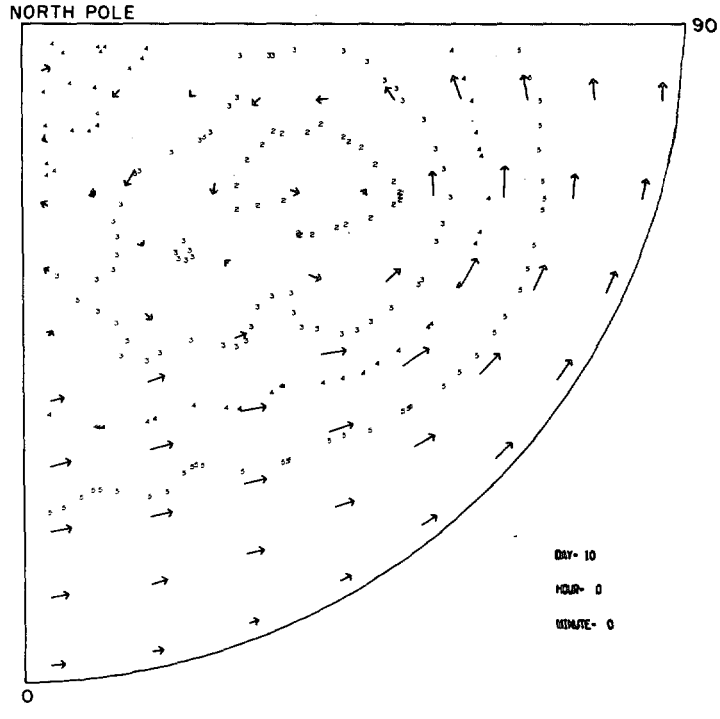

FIGURE 3.—Forecast height and wind fields at the end of the 10th day for experiment 2. Legend for contour values in figure 1.

a tendency to level off. The rate of increase and the absolute increase of the global kinetic energy shows an inverse relation to the resolution.

Finally, figure 14 exhibits the effects of different resolutions clearly. First, the irregularities in the mean zonal wind north of the 50° latitude belt bear an inverse relationship with the resolution. Second, the mean zonal wind shear in the middle latitudes also bears an inverse relationship with the resolution, with easterlies appearing for $N=20$, 36, and 48. Grimmer and Shaw (1967) observed the same behavior with the VDL scheme for $N=20$. For $N=72$, the zonal wind profile approaches that of the previous results of Kurihara (1965), runs 1, 11, and 12.

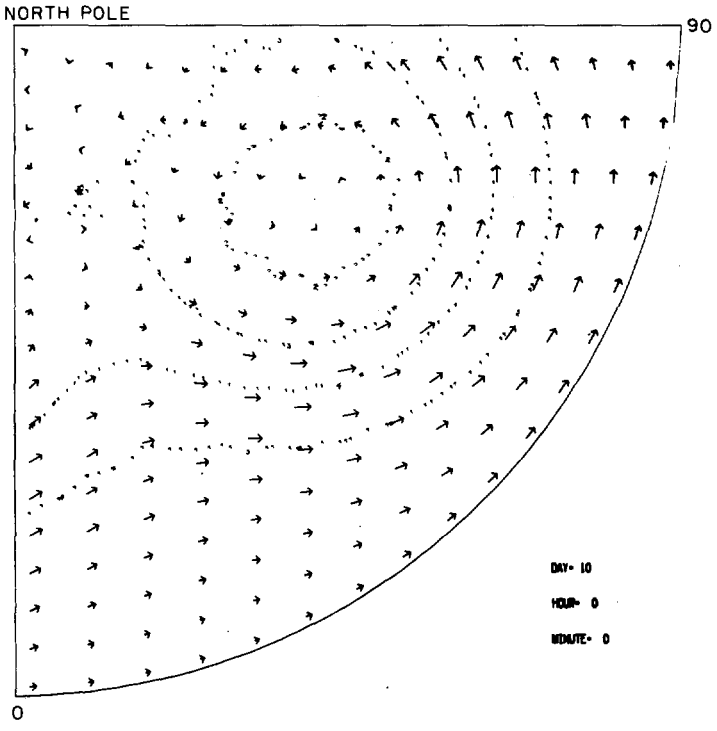

FIGURE 4.—Forecast height and wind fields at the end of the 10th day for experiment 3. Legend for contour values in figure 1.

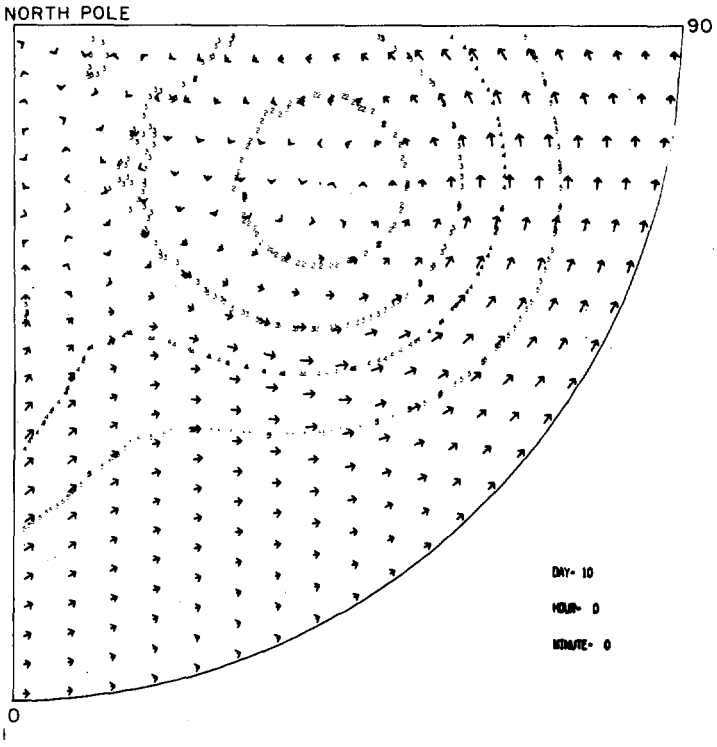

FIGURE 6.—Forecast height and wind fields at the end of the 10th day for experiment 5. Legend for contour values in figure 1.

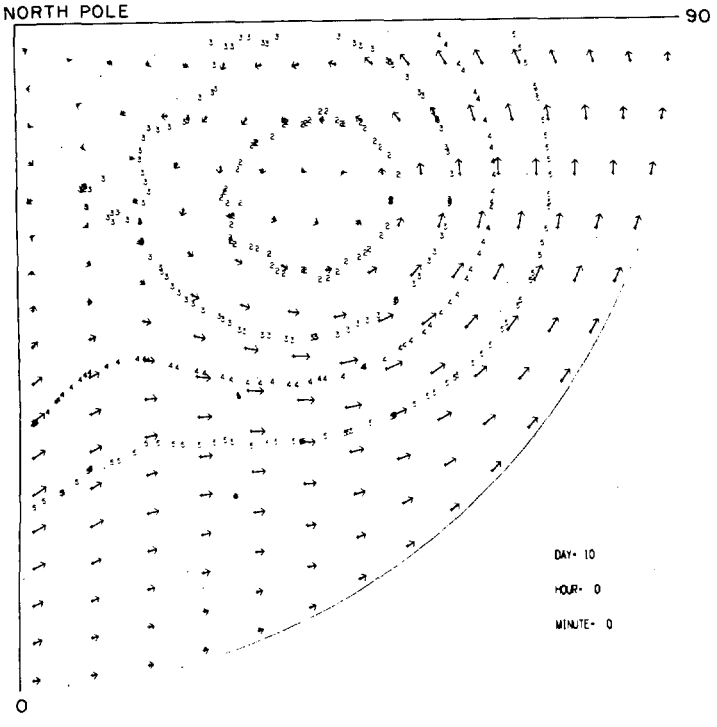

FIGURE 5.—Forecast height and wind fields at the end of the 10th day for experiment 4. Legend for contour values in figure 1.

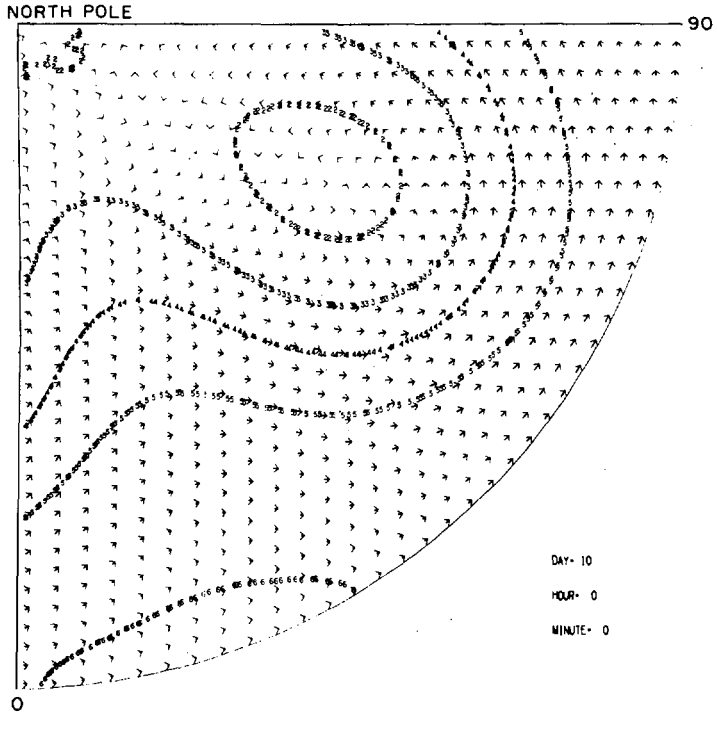

FIGURE 7.—Forecast height and wind fields at the end of the 10th day for experiment 6. Legend for contour values in figure 1.

In experiments 7 and 8, we added to the $N=20$ grid an equal number of additional points at every latitude. Thus, in experiment 7, we have nine points per octant near the Pole, while in experiment 8, we have 15 points per octant near the Pole, instead of one point per octant as in the usual homogeneous grid.

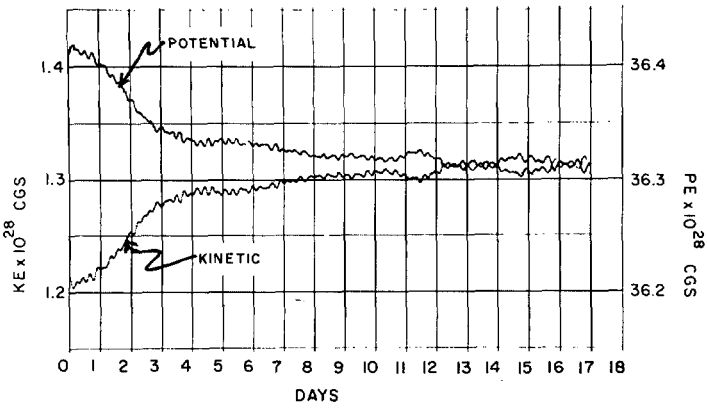

FIGURE 8.—Kinetic and potential energies over the entire octant for the total period of integration, experiment 1.

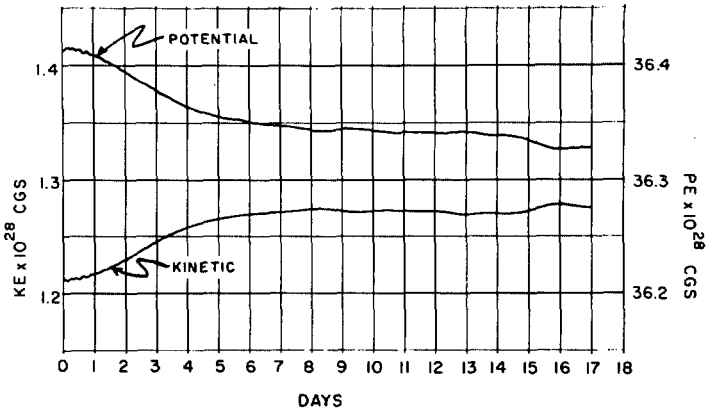

FIGURE 11.—Kinetic and potential energies over the entire octant for the total period of integration, experiment 4.

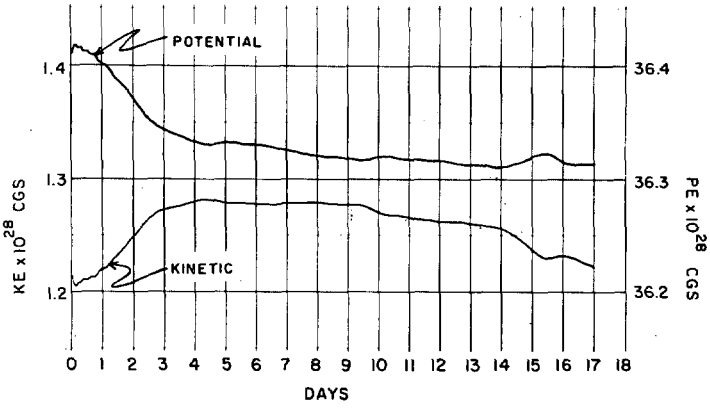

FIGURE 9.—Kinetic and potential energies over the entire octant for the total period of integration, experiment 2.

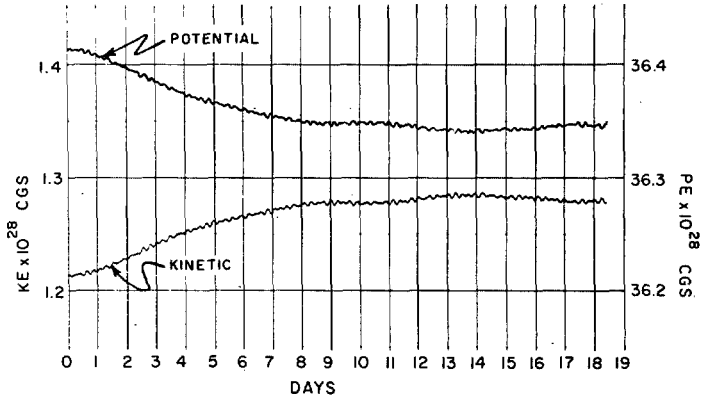

FIGURE 12.—Kinetic and potential energies over the entire octant for the total period of integration, experiment 5.

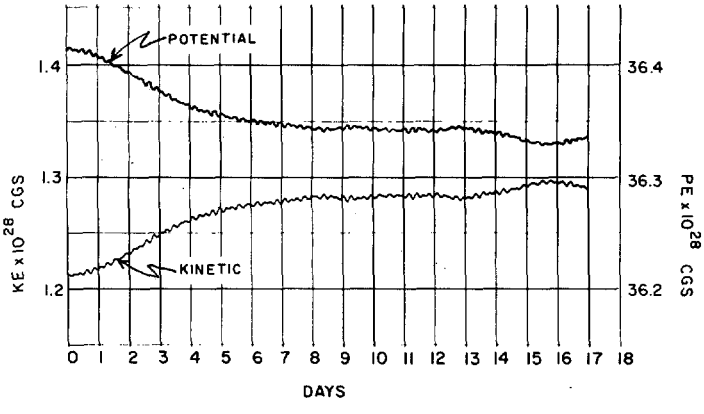

FIGURE 10.—Kinetic and potential energies over the entire octant for the total period of integration, experiment 3.

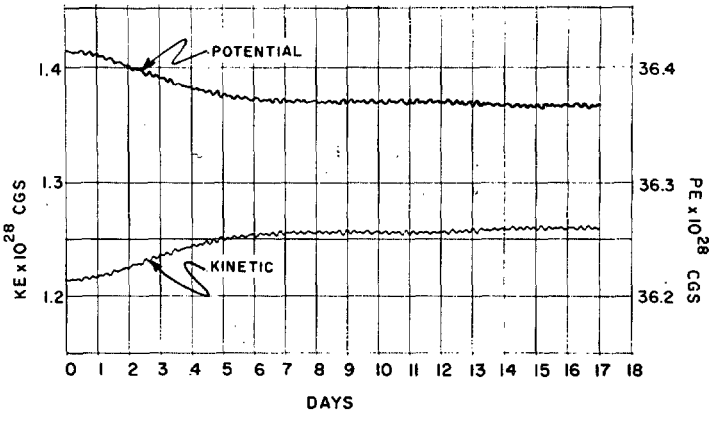

FIGURE 13.—Kinetic and potential energies over the entire octant for the total period of integration, experiment 6.

Corresponding results are given in figures 15 to 19. From these, as well as from table 1, cases 7 and 8, it can be seen that there is a marked improvement in the results although the number of grid points for the entire octant and at low latitudes in these experiments is less than for $N=48$ or $N=72$.

Experimenting with real data, Gerrity and Dey (1969) also arrived at similar results. Future experiments are

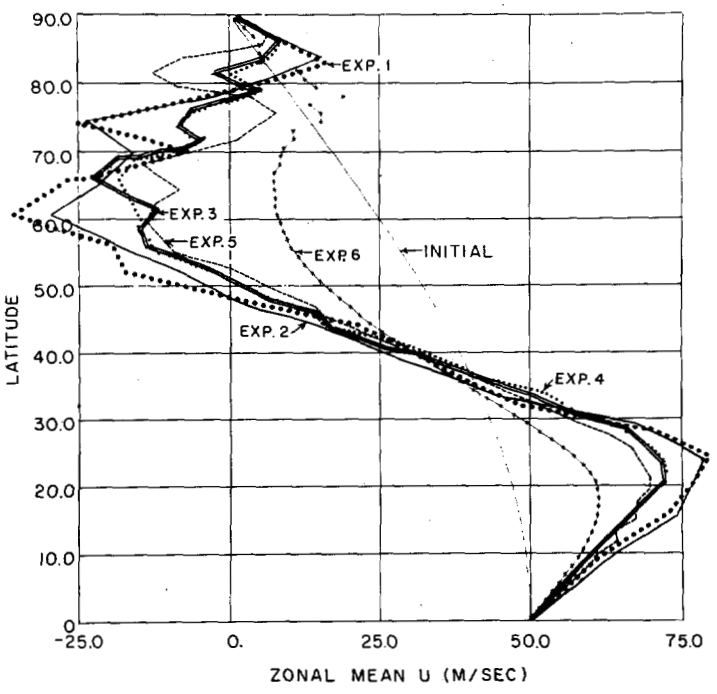

FIGURE 14.—Zonal mean velocity for experiments 1–6 at the end of the 10th day.

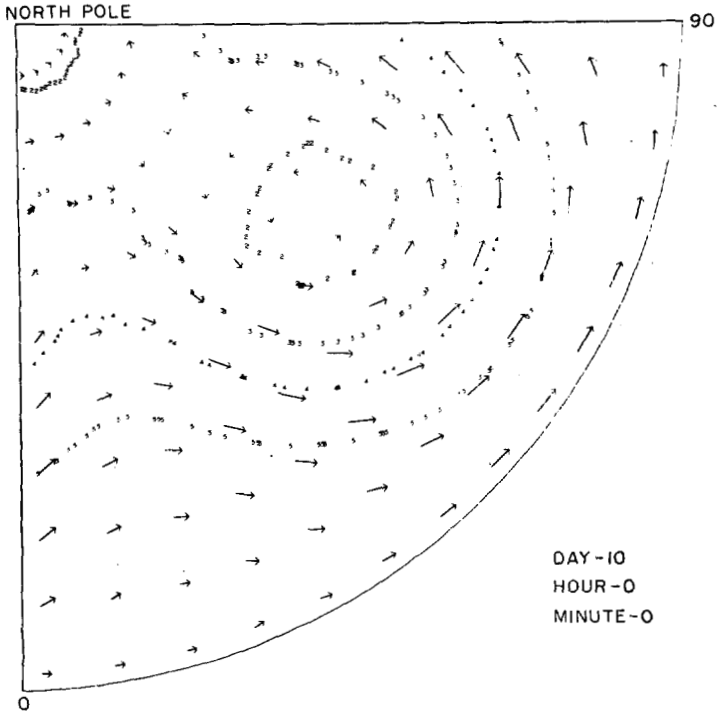

FIGURE 15.—Forecast height and wind fields at the end of the 10th day for experiment 7. Legend for contour values in figure 1.

planned with a grid having adequate resolution near the polar latitudes.

ACKNOWLEDGMENTS

M. Sankar Rao thanks the National Academy of Sciences for the opportunity to conduct research on the problems of planetary

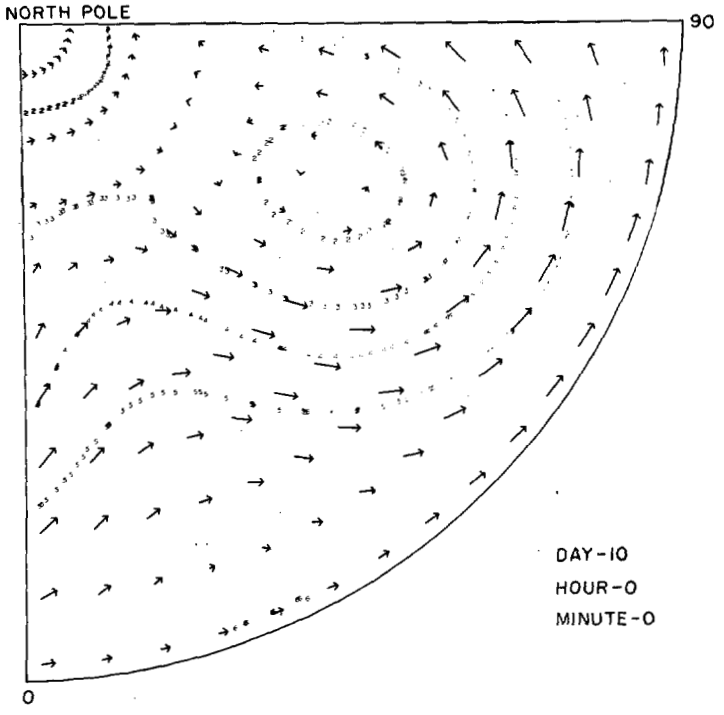

FIGURE 16.—Forecast height and wind fields at the end of the 10th day for experiment 8. Legend for contour values in figure 1.

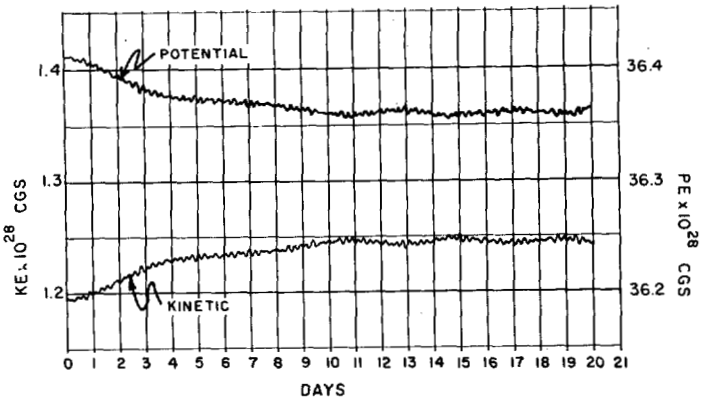

FIGURE 17.—Kinetic and potential energies over the entire octant for the total period of integration, experiment 7.

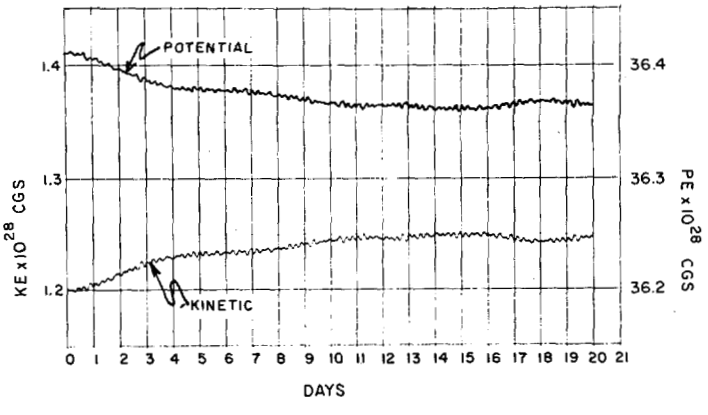

FIGURE 18.—Kinetic and potential energies over the entire octant for the total period of integration, experiment 8.

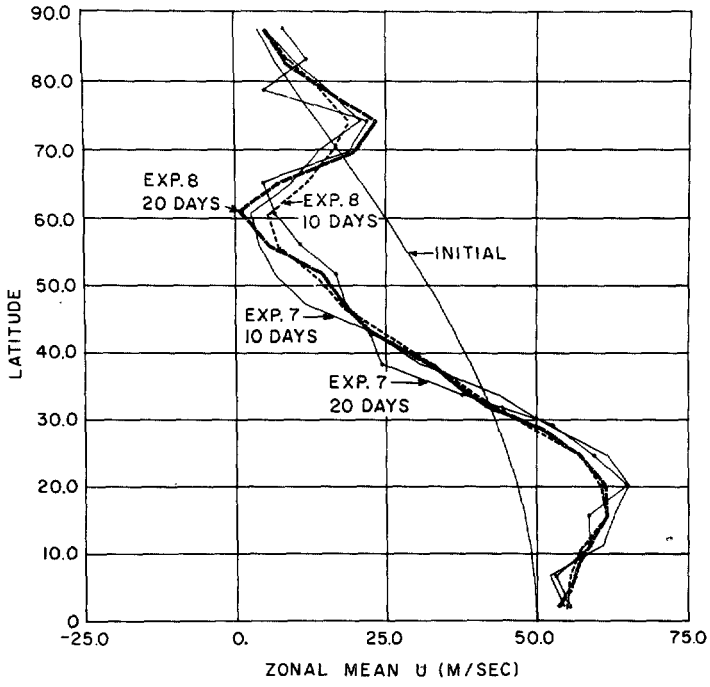

FIGURE 19.—Zonal mean velocity for experiments 7 and 8 at the end of the 10th and 20th days.

climates at The Institute for Space Studies, New York. The authors wish to thank Dr. Robert Jastrow for his critical interest in this work.

REFERENCES

Charney, J. G., "The Use of Primitive Equations of Motion in Numerical Prediction," *Tellus*, Vol. 7, No. 1, Feb. **1955**, pp. 22–26.

Gerrity, J. P., Jr., and Dey, C., "Some Real Data Experiments With the Kurihara Global Grid," paper presented at the 49th Annual Meeting of the American Meteorological Society, New York City, Jan. 20–23, **1969**.

Grimmer, M., and Shaw, D. G., "Energy-Preserving Integrations of the Primitive Equations on the Sphere," *Quarterly Journal of the Royal Meteorological Society*, Vol. 93, No. 397, July **1967**, pp. 337–349.

Haurwitz, B., "The Motion of Atmospheric Disturbances on the Spherical Earth," *Journal of Marine Research*, Vol. III, No. 3, **1940**, pp. 254–267.

Kurihara, Y., "Numerical Integration of Primitive Equations on a Spherical Grid," *Monthly Weather Review*, Vol. 93, No. 7, July **1965**, pp. 399–415.

Kurihara, Y., and Holloway, J. L., Jr., "Numerical Integration of a Nine-Level Global Primitive Equations Model Formulated by the Box Method," *Monthly Weather Review*, Vol. 95, No. 8, Aug. **1967**, pp. 509–530.

Phillips, N. A., "Numerical Integration of the Primitive Equations on the Hemisphere," *Monthly Weather Review*, Vol. 87, No. 9, Sept. **1959**, pp. 333–345.

[*Received January 28, 1969; revised May 15, 1969*]